

# The formation of Schrodinger cat-like states in the process of spontaneous parametric down-conversion

Ranjit Singh\*

*Independent Researcher, Domodedovo, 142000, Moscow region, Russia*

Alexander E. Teretenkov†

*Department of Mathematical Methods for Quantum Technologies,  
Steklov Mathematical Institute of Russian Academy of Sciences, 8 Gubkina St., Moscow, 119991, Russia*

(Dated: November 26, 2024)

We show the formation of Schrodinger cat-like states (SCLSs) during the spontaneous parametric down-conversion (SPDC) process when the pump mode is considered quantum and depleted. For the first time, we show the formation of SCLSs in the fundamental and second harmonic modes under non-dissipative and dissipative regimes. The Wigner function is used to visualize qualitatively SCLSs. We have performed quantitative analysis of SCLSs by calculating values of the mean number of photon, photon number distribution, the variance of quadrature component, the Fano factor and fidelity.

## I. INTRODUCTION

Schrodinger cat states or even and odd coherent states [1] with the negative value of the Wigner function play an important role e.g., in the observing phase displacements as they are very sensitive to the phase change [2–5]. Usually Schrodinger cat states [1], Fock states, photon added, subtracted states show non-Gaussianity (negative value of the Wigner function in the phase space) [6]. Schrodinger cat states can be used to encode cat qubits [7] and to build Ising machines [8]. This is due to the fact that such qubits can be created using a single mode. Moreover, Schrodinger cat states have the sub-Planck structure (interference pattern between macroscopically distinct states) in phase space [9].

In the field of quantum nonlinear optics, the generation of non-Gaussian states requires at least the cubic form of the interaction Hamiltonian [10]. The formation of non-Gaussian states [11] (e.g., SCLSs) was considered in [12, 13] during the quantum state evolution of the fundamental mode in the process of second harmonic generation in the nonlinear medium with non-zero second order susceptibility  $\chi^{(2)}$ . In [12] the interference pattern between superposition of macroscopically distinct states is absent because the Husimi function was used to study the phase-space portraits. Later in [13] presence of the interference pattern between superposition of two macroscopically distinct states was observed in the fundamental mode in the process of second harmonic generation by using the Wigner function. The generation of Schrodinger cat states has also been studied by using the combination of squeezed states and linear optics [11, 14, 15], photon added and subtracted states by addition and subtraction of photons on Gaussian states [6], in the Kerr medium ( $\chi^{(3)}$ ) and the cubic phase [16–18].

Usually, nonlinear processes in quantum nonlinear optics were studied by considering the undepleted classical pump-mode approach, i.e. by using the semi-classical method [6, 19]. This method approximates the interaction Hamiltonian for the SPDC process based on  $\chi^{(2)}$ , which is cubic, by a quadratic one. Such an approximation neglects the non-Gaussianity features (negative value of the Wigner function) present in the initial cubic form of the interaction Hamiltonian. Another approximation method, e.g., expansion of unitary operators [20–22] can be applied to consider full treatment of quantum effects present in all modes of the SPDC process. Such an approximation method is in good agreement at very early stages of evolution and starts to deviate at later stages [22]. However, the diagonalization method [22–26] can be used to study evolution at longer interaction lengths without losing the quantum effects present in the interacting modes.

One can also find a number of papers where the full quantum mechanical approach is used by considering the quantum depleted pump mode [23–28] in the SPDC. In these papers, quantum statistical properties such as the mean number of photons, the phase, the quadrature components of modes and their fluctuations of the fundamental mode and phase properties of the second harmonic mode [29] in the SPDC process were studied.

In this paper, we have studied the formation of SCLSs for two cases (non-dissipative and dissipative) when both modes (fundamental and second harmonic) are considered as quantum and depleted during the effective realization of the SPDC process based on  $\chi^{(2)}$  [6, 19]. QuTiP [30, 31] is used to numerically solve the Lindbladian superoperator responsible for the SPDC process. The formation of SCLSs is studied and illustrated qualitatively using the Wigner function. Quantitative analysis of the SCLSs is performed by calculating values of the mean number of photons, photon number distributions, the variance of quadrature components, the Fano factor and fidelity. The SCLSs are observed in the fundamental and

---

\* ranjit.singh@mail.ru

† taemsu@mail.ru

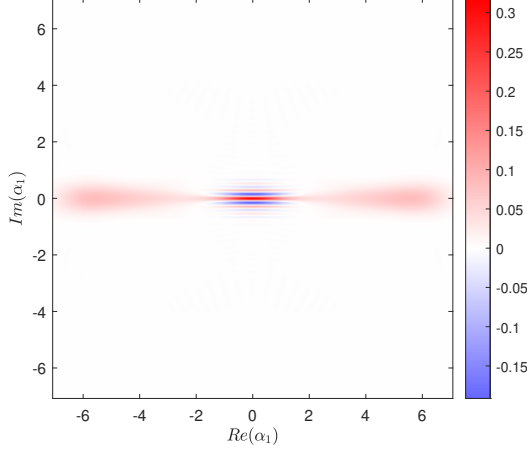


FIG. 1. Non-dissipative case ( $\gamma_{1,2} = 0$ ). Wigner function  $W_1(\alpha_1, \tau)$  of formation of the SCLS of mode  $\hat{a}_1$  during the SPDC process at normalized interaction length  $\tau = 0.38$  and  $n_1 \approx 25.2$ . At  $\tau = 0$  fundamental mode  $\hat{a}_1$  is in the vacuum state, pump mode  $\hat{a}_2$  - in the coherent state and  $|\alpha_{20}|^2 = 20, \varphi_{20} = \pi/2$  at the input of the nonlinear crystal.

second harmonic modes for both cases when the fundamental mode is in the vacuum state and the second harmonic mode is in the coherent state.

## II. INTERACTION HAMILTONIAN AND LINDBLADIAN

Let three stationary degenerate monochromatic optical plane wave modes  $\hat{a}_s, \hat{a}_i, \hat{a}_p$  of frequencies  $\omega_s^o, \omega_i^o, \omega_p^e$  propagate collinearly in a nonlinear optical crystal with non-zero susceptibility  $\chi^{(2)}$ . Superscripts  $o, e$  belong to the ordinary and extraordinary polarization of the respective modes. Subscripts  $i, s, p$  belong to the idler, signal, and pump modes. In case of degenerate frequencies:  $\omega_s^o = \omega_i^o = \omega, \omega_p^e = 2\omega, \hat{a}_i = \hat{a}_s = \hat{a}_1, \hat{a}_p = \hat{a}_2$ . For effective realization of the SPDC process, it is assumed that all three modes can be phase-matched [32]. The interaction Hamiltonian of the SPDC process ( $2\omega = \omega + \omega$ ) [6, 19] is given by

$$\hat{H}_{int} = \hbar g (\hat{a}_1^2 \hat{a}_2^\dagger + h.c.), \quad (1)$$

where  $\hbar$  is the Planck constant. For simplicity  $\hbar = 1$ .  $g$  is the nonlinear coupling constant of the interacting modes.

The Lindblad master equation for the density matrix  $\hat{\rho}$  describing an open quantum system is used to study the quantum dynamics of the interaction Hamiltonian (1) and can be written as [6, 19, 33–35]

$$\frac{d\hat{\rho}}{d\tau} = -ig^{-1}[\hat{H}_{int}, \hat{\rho}] + \sum_{j=1}^2 \left( \hat{C}_j \hat{\rho} \hat{C}_j^\dagger - \frac{1}{2} \{ \hat{C}_j^\dagger \hat{C}_j, \hat{\rho} \} \right), \quad (2)$$

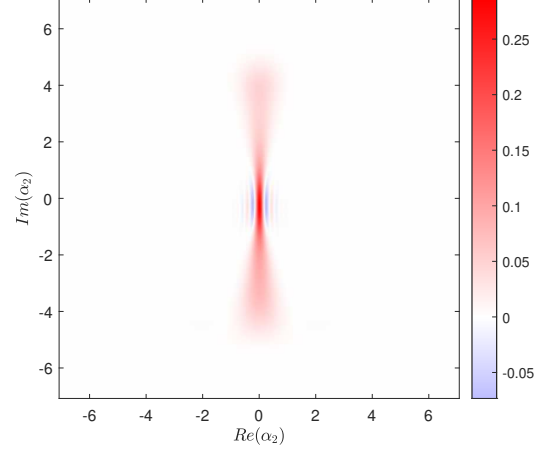


FIG. 2. Non-dissipative case ( $\gamma_{1,2} = 0$ ). Wigner function  $W_2(\alpha_2, \tau)$  of formation of the SCLS of mode  $\hat{a}_2$  during the SPDC process at normalized interaction length  $\tau = 0.38$  and  $n_2 \approx 7.3$ . At  $\tau = 0$  fundamental mode  $\hat{a}_1$  is in the vacuum state, pump mode  $\hat{a}_2$  - in the coherent state and  $|\alpha_{20}|^2 = 20, \varphi_{20} = \pi/2$  at the input of the nonlinear crystal.

where  $\tau = gt$  is the normalized interaction length.  $\hat{C}_j = \sqrt{\gamma_j/g} \hat{a}_i$  are the Lindblad operators describing the dissipative part of the dynamics, where  $\gamma_j \geq 0$  are the cavity damping rates of the modes and  $g > 0$ .

Equation (2) is numerically solved by using QuTiP for two cases (non-dissipative  $\gamma_j = 0$  and dissipative  $\gamma_j = 0.1$ ) for the initial state density matrix  $\hat{\rho}(0) = |\psi_0\rangle\langle\psi_0|$ . At the input of the nonlinear crystal, the fundamental mode is in the vacuum state  $|0\rangle_1$ , the second harmonic one is in the coherent state  $|\alpha_{20}\rangle_2 = e^{-|\alpha_{20}|^2/2} \sum_{n_2=0}^{\infty} \frac{\alpha_{20}^{n_2}}{\sqrt{n_2!}} |n_2\rangle$ , having mean number of photons  $|\alpha_{20}|^2 = 20$  and phase  $\varphi_{20} = \pi/2$ , i.e.,  $|\psi_0\rangle = |0\rangle_1 \otimes |\alpha_{20}\rangle_2$ .

## III. WIGNER FUNCTION

One can study and analyze the quantum statistical properties of the modes by using the Wigner quasiprobability distribution [6, 19]. Phase space portraits of the Wigner function help to visualize delicate patterns, such as (a) interference (wave nature) present in the superposition of macroscopically distinct states, e.g., SCLSs, (b) non-Gaussianity of the state, i.e., the negative value of the Wigner function. The Wigner functions of the modes  $\hat{a}_1$  and  $\hat{a}_2$  are calculated using

$$W_j(\alpha_j, \tau) = \frac{1}{\pi} \int_{-\infty}^{\infty} \langle \Re(\alpha_j) - y | \hat{\rho}_j(\tau) | \Re(\alpha_j) + y \rangle e^{2i\Im(\alpha_j)y} dy, \quad (3)$$

where  $j = 1, 2, \hat{\rho}_1(\tau) = \text{Tr}_2[\hat{\rho}(\tau)], \hat{\rho}_2(\tau) = \text{Tr}_1[\hat{\rho}(\tau)]$  are reduced density matrices of states of the modes  $\hat{a}_1$  and

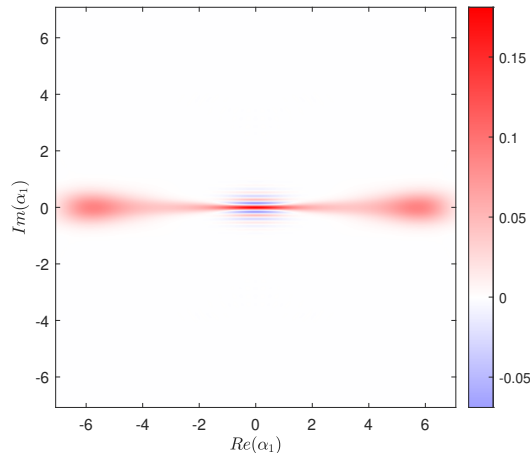


FIG. 3. Dissipative case ( $\gamma_{1,2} = 0.1$ ). Wigner function  $W_1(\alpha_1, \tau)$  of formation of the SCLS of mode  $\hat{a}_1$  during the SPDC process at normalized interaction length  $\tau = 0.38$  and  $n_1 \approx 24.34$ . At  $\tau = 0$  fundamental mode  $\hat{a}_1$  is in the vacuum state, pump mode  $\hat{a}_2$  - in the coherent state and  $|\alpha_{20}|^2 = 20, \varphi_{20} = \pi/2$  at the input of the nonlinear crystal.

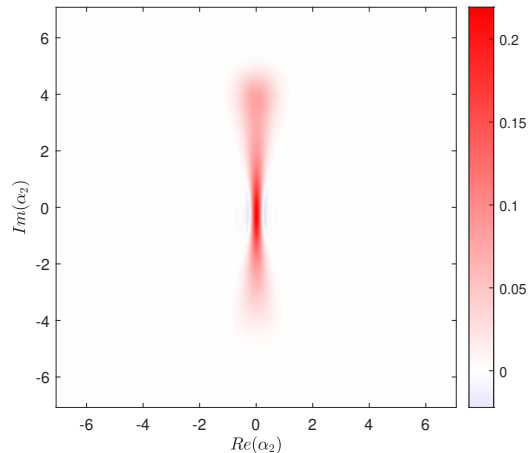


FIG. 4. Dissipative case ( $\gamma_{1,2} = 0.1$ ). Wigner function  $W_2(\alpha_2, \tau)$  of formation of the SCLS of mode  $\hat{a}_2$  during the SPDC process at normalized interaction length  $\tau = 0.38$  and  $n_2 \approx 7.08$ . At  $\tau = 0$  fundamental mode  $\hat{a}_1$  is in the vacuum state, pump mode  $\hat{a}_2$  - in the coherent state and  $|\alpha_{20}|^2 = 20, \varphi_{20} = \pi/2$  at the input of the nonlinear crystal.

$\hat{a}_2$ .

In Fig. 1-4 plots of (3) are shown for two cases (non-dissipative and dissipative) of the formation of SCLSs in the fundamental and second harmonic modes.

#### IV. SOME QUANTUM STATISTICAL PROPERTIES OF SCLSS

Using the Wigner function, we calculated the contribution of all statistical moments present in the SCLSs and qualitatively visualized portraits of the Wigner functions in phase space (see Fig. 1-4). In order to quantitatively estimate quantum statistical properties such as mean number of photons, photon number distribution, squeezing level (the variances of quadrature components, the Fano factor) and fidelity of quantum states (closeness of SCLSs to squeezed Schrodinger cat states), additional calculations are performed.

##### A. Mean number of photons and variances of the quadrature components

The mean number of photons in the both modes  $\hat{a}_j$  is calculated using

$$n_j(\tau) = \text{Tr}[\hat{a}_j^\dagger \hat{a}_j \hat{\rho}_j(\tau)]. \quad (4)$$

The variances of the quadrature components are calculated using

$$\Delta^2 x_j = \text{Tr}[\hat{x}_j^2 \hat{\rho}_j(\tau)] - \text{Tr}[\hat{x}_j \hat{\rho}_j(\tau)]^2, \quad (5)$$

$$\Delta^2 p_j = \text{Tr}[\hat{p}_j^2 \hat{\rho}_j(\tau)] - \text{Tr}[\hat{p}_j \hat{\rho}_j(\tau)]^2, \quad (6)$$

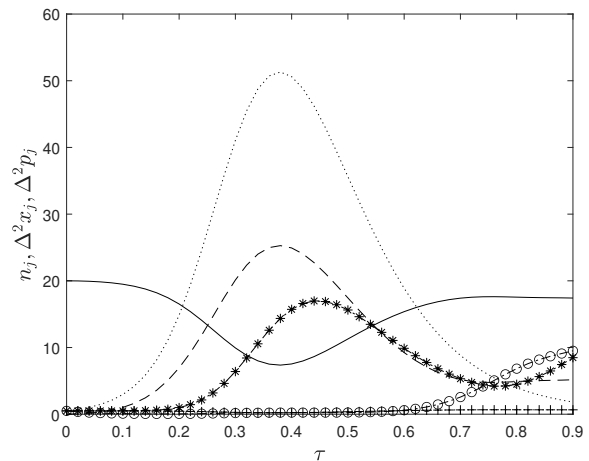


FIG. 5. Mean number of photons and variances of quadrature components of modes  $\hat{a}_j$ . Solid (—) and dotted (---) lines correspond to the mean number of photons in the fundamental  $\hat{a}_1$  and the second harmonic  $\hat{a}_2$  modes. Variances of the quadrature components  $\Delta^2 x_1$  and  $\Delta^2 p_1$  of the mode  $\hat{a}_1$  are represented by dots (.) and markers (o). Variances of the quadrature components  $\Delta^2 x_2$  and  $\Delta^2 p_2$  of the mode  $\hat{a}_2$  are represented by the markers (+) and (\*).

where  $\hat{x}_j = 2^{-(1/2)}(\hat{a}_j + \hat{a}_j^\dagger)$  and  $\hat{p}_j = -i2^{-(1/2)}(\hat{a}_j - \hat{a}_j^\dagger)$  are the quadrature components of the modes  $\hat{a}_j$ . Fig. 5 shows the evolution of the mean number of photons (4) and the variances of the quadrature components (5,6) of the modes  $\hat{a}_j$  for the non-dissipative case. SCLSs are formed at the first maximum and minimum values of the mean number of photons of modes  $\hat{a}_1$  and  $\hat{a}_2$ . Note that the variances of the quadrature components  $\Delta^2 p_1 = 0.23$

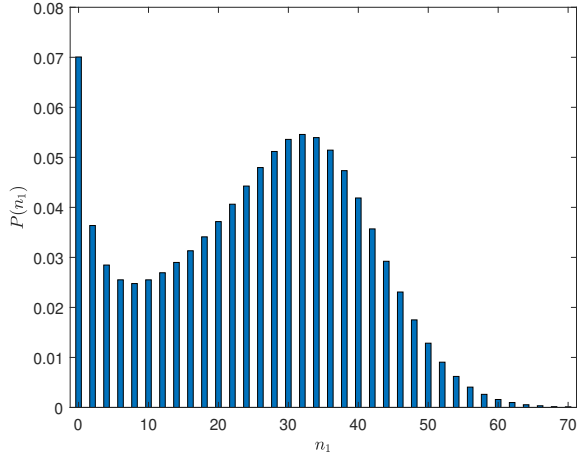


FIG. 6. Non-dissipative case ( $\gamma_{1,2} = 0$ ). Photon number distribution  $P(n_1)$  of mode  $\hat{a}_1$ .

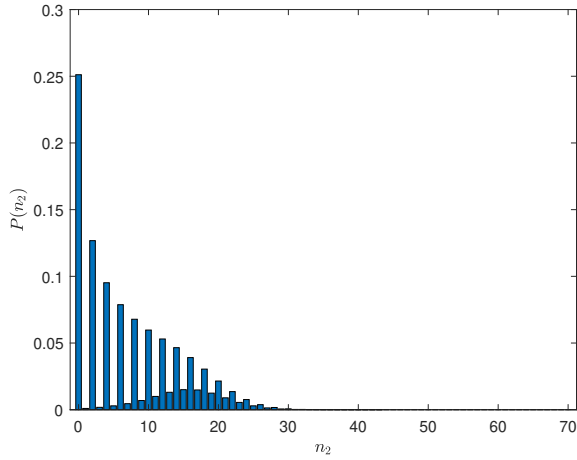


FIG. 7. Non-dissipative case ( $\gamma_{1,2} = 0$ ). Photon number distribution  $P(n_2)$  of mode  $\hat{a}_2$ .

and  $\Delta^2 x_2 = 0.21$  of the modes  $\hat{a}_1$  and  $\hat{a}_2$  are squeezed, i.e. 7.37 dB and 8.39 dB.

### B. Fano factor

The value of the Fano factor can identify the type (sub-Poissonian, Poissonian, super-Poissonian) of the distributions of the studied SCLS  $\hat{\rho}_j$ . Thus, the Fano factor [36] is calculated using

$$FF_j(\tau) = \frac{\text{Tr}[(\hat{a}_j^\dagger \hat{a}_j)^2 \hat{\rho}_j(\tau)] - n_j^2(\tau)}{n_j(\tau)}. \quad (7)$$

Fano factors  $FF_j$  can take three values: if  $FF_j < 1$ , then the mode states belong to the sub-Poissonian distribution, if  $FF_j = 1$ , then the mode states belong

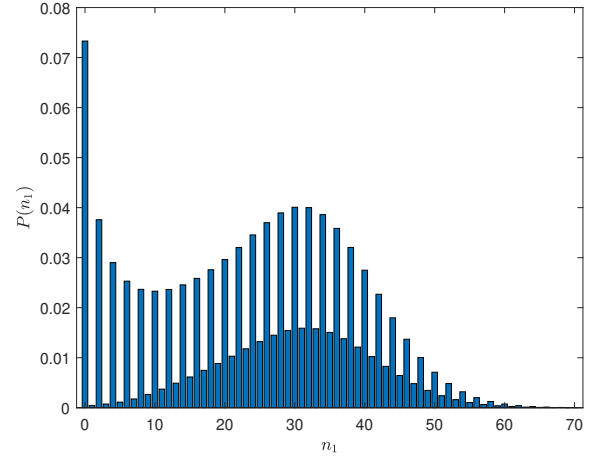


FIG. 8. Dissipative case ( $\gamma_{1,2} = 0.1$ ). Photon number distribution  $P(n_1)$  of mode  $\hat{a}_1$ .

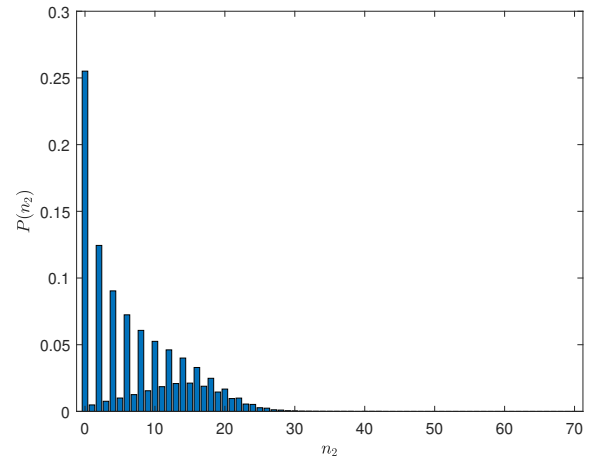


FIG. 9. Non-dissipative case ( $\gamma_{1,2} = 0.1$ ). Photon number distribution  $P(n_2)$  of mode  $\hat{a}_2$ .

to the Poissonian distribution, and  $FF_j > 1$ , then the mode states belong to the super-Poissonian distribution. The Fano factor (7) at  $\tau = 0.38$  is calculated for non-dissipative and dissipative cases.

$$FF_j(0.38) = \begin{cases} 8.54, & j = 1, & \text{super-Poissonian, non-dissipative} \\ 8.41, & j = 1, & \text{super-Poissonian, dissipative} \\ 6.67, & j = 2, & \text{super-Poissonian, non-dissipative} \\ 6.48, & j = 2, & \text{super-Poissonian, dissipative} \end{cases} \quad (8)$$

### C. Photon number distribution

Another informative quantum statistical property of SCLSs  $\hat{\rho}_j$  is the photon number distribution. It helps to identify the type of pattern an SCLS belongs to, e.g. even, odd, mixture of even and odd coherent states. The photon number distribution is calculated using

$$P_j(n) = \text{Tr}[\hat{\rho}_j|n\rangle\langle n|], \quad (9)$$

Figs. 6-9 show pattern types of photon number distributions of SCLSs  $\hat{\rho}_j$ . In case of non-dissipative regime, photon number distributions of SCLSs  $\hat{\rho}_j$  for modes  $\hat{a}_1$  and  $\hat{a}_2$  are associated with even and mixture of even and odd coherent states. In the case of the dissipative regime, Figs. 8-9 show that the SCLSs  $\hat{\rho}_j(\tau)$  are associated with the photon number distribution of the mixture of even and odd coherent states. The dissipative regime introduces an odd number of photons into the SCLSs  $\hat{\rho}_j(\tau)$  (see Figs. 8-9).

### D. Fidelity of SCLSs

The fidelity of SCLSs shows the closeness of two density matrices [37]. In our case we quantify the fidelity of reduced density matrices  $\hat{\rho}_j$  of SCLSs of modes  $\hat{a}_j$  to density matrices of squeezed even  $\hat{\sigma}_j$  coherent states. The fidelity is calculated with

$$F_j(\hat{\rho}_j, \hat{\sigma}_j) = \left( \text{Tr} \sqrt{\sqrt{\hat{\rho}_j} \hat{\sigma}_j \sqrt{\hat{\rho}_j}} \right)^2, \quad (10)$$

## V. SUMMARY AND CONCLUSIONS

We have shown the formation of SCLSs during the realization of the SPDC process when both modes are considered quantum and depleted under non-dissipative

where  $\hat{\sigma}_j = \hat{S}_j|\alpha_+^{(j)}\rangle\langle\alpha_+^{(j)}|\hat{S}_j^\dagger$ ,  $\hat{S}_j = \exp(-i\tilde{\tau}(e^{-i\tilde{\varphi}_b^{(j)}}\hat{a}_1^2 + h.c.))$  is the squeeze operator and is obtained by replacing  $\hat{a}_2$  in (1) by the c-number  $|B|e^{i\tilde{\varphi}_b^{(j)}}$ .  $\tilde{\varphi}_b^{(j)} = (-1)^{j-1}\pi/2$ .  $\tilde{\tau} = g|B|t$  is the normalized interaction length.  $|\alpha_+^{(j)}\rangle = (\mathcal{N}^{(j)})^{-1}(|e^{i(j-1)\frac{\pi}{2}}\tilde{\alpha}_0^{(j)}\rangle + |-e^{i(j-1)\frac{\pi}{2}}\tilde{\alpha}_0^{(j)}\rangle)$  is the even coherent state [1].  $\tilde{\alpha}_0^{(j)} = |\tilde{\alpha}_0^{(j)}|e^{i\tilde{\varphi}_0^{(j)}}$ .  $\tilde{\varphi}_0^{(j)} = 0$ .  $\mathcal{N}^{(j)} = \sqrt{2(1 + e^{-2|\tilde{\alpha}_0^{(j)}|^2})}$  is the normalization constant.

Mean number of photons for the even coherent state  $\hat{\sigma}_j$  is calculated using [5]

$$\begin{aligned} \tilde{n}_j(\tilde{\tau}) &= \text{Tr}[\hat{a}_1^\dagger \hat{a}_1 \hat{\sigma}_j] \\ &= 2^{-1}(-1 + 2|\tilde{\alpha}_0^{(j)}|^2 \sinh(4\tilde{\tau}) \\ &\quad + \cosh(4\tilde{\tau}) (1 + 2|\tilde{\alpha}_0^{(j)}|^2 \tanh(|\tilde{\alpha}_0^{(j)}|^2)) \chi(11) \end{aligned}$$

For the calculation of the optimal value of (10) the mean number of photons (4) of the SCLSs  $\hat{\rho}_j$  for non-dissipative and dissipative cases are set equal to the mean number of photons (11) of the even coherent state  $\hat{\sigma}_j$ , i.e.,

$$\tilde{n}_j(\tilde{\tau}) = n_j(\tau). \quad (12)$$

From equation (12) the set of values  $\tilde{\tau}$  and  $|\tilde{\alpha}_0^{(j)}|^2$  is calculated numerically. The obtained set of values  $\tilde{\tau}$ ,  $|\tilde{\alpha}_0^{(j)}|^2$  are used to find maximum values of fidelity when  $\tau = 0.38$ , i.e.,

$$F_1(\hat{\rho}_1, \hat{\sigma}_1) = \begin{cases} 0.78, & n_1 \approx 25.27, \tilde{\tau} = 0.33, & |\tilde{\alpha}_0^{(1)}|^2 \approx 6.61 & \text{non-dissipative} \\ 0.68, & n_1 \approx 24.34, \tilde{\tau} = 0.33, & |\tilde{\alpha}_0^{(1)}|^2 \approx 6.36 & \text{dissipative} \end{cases} \quad (13)$$

$$F_2(\hat{\rho}_2, \hat{\sigma}_2) = \begin{cases} 0.79, & n_2 \approx 7.36, \tilde{\tau} = 0.36, & |\tilde{\alpha}_0^{(2)}|^2 \approx 1.65 & \text{non-dissipative} \\ 0.77, & n_2 \approx 7.08, \tilde{\tau} = 0.45, & |\tilde{\alpha}_0^{(2)}|^2 \approx 1.1 & \text{dissipative} \end{cases} \quad (14)$$

and dissipative regimes. The formation of such states is studied qualitatively by visualizing the values of the Wigner functions for both modes. At  $\tau = 0$  the fundamental and second harmonic modes at the input of the nonlinear crystal are in the vacuum state and in the co-

herent state (with mean number of photons and phase  $|\alpha_{20}|^2 = 20, \varphi_{20} = \pi/2$ ).

The plot of (3) (see Fig. 1) shows the formation of the SCLS of the mode  $\hat{a}_1$  at interaction length  $\tau = 0.38$  and mean number of photons  $n_1 \approx 25.2$  for the non-dissipative case ( $\gamma_{1,2} = 0$ ). At the same normalized interaction length  $\tau = 0.38$ , the plot of (3) (see Fig. 2) shows the formation of an SCLS in the mode  $\hat{a}_2$  and with a mean number of photons  $n_2 \approx 7.3$ . The interference pattern in Fig. 2 shows the presence of a superposition of macroscopic states in the  $\hat{a}_2$  mode.

For the dissipative case, ( $\gamma_{1,2} = 0.1$ ) the same interaction length  $\tau = 0.38$  and initial conditions as for the non-dissipative case ( $\gamma_{1,2} = 0$ ) are considered. The plot of (3) (see Fig. 3 and Fig. 4) shows the lower number of photons in the formed SCLSs compared to the non-dissipative case (see Fig. 1 and Fig. 2). In addition, the pattern of SCLSs formed in the dissipative case is visually significantly preserved compared to the non-dissipative case and shows non-Gaussianity (the value of the Wigner function is negative).

Analysis of the evolution of the mean number of photons and the variances of the quadrature components (see Fig. 5) shows that SCLSs are formed at the first maximum and minimum values of the mean number of photons of modes  $\hat{a}_1$  and  $\hat{a}_2$ . The variances of the quadrature components  $\Delta^2 p_1 = 0.23$  ( $\approx 7.2$  dB) and  $\Delta^2 x_2 = 0.21$  ( $\approx 8.3$  dB) of the SCLSs are squeezed.

The values of the Fano factors show that both modes  $\hat{a}_j$  statistics become super-Poissonian (8). This may help to identify the measurement method, i.e, whether to use photon number resolving detectors (PNRD) [38] to identify even, odd coherent states or quantum optical homodyne tomography [39].

The fidelity values for the non-dissipative case (13,14) of the SCLSs of modes  $\hat{a}_1$  and  $\hat{a}_2$  are 0.78 and 0.79 and for the dissipative case 0.68 and 0.77. The effect of the dissipation on the SCLSs reduces the non-Gaussianity (negative value of the Wigner function in the phase space) by about 13% in the case of the mode  $\hat{a}_1$  and by about 3%

in the case of the mode  $\hat{a}_2$ .

To generate an odd SCLS, one can change the initial state for both cases (non-dissipative and dissipative) from  $|\psi_0\rangle = |0\rangle_1 \otimes |\alpha_{20}\rangle_2$  to  $|\psi_0\rangle = |1\rangle_1 \otimes |\alpha_{20}\rangle_2$ . It is easy to see that only an odd number of photons is present in the state  $e^{-itg\hat{H}_{int}}|1\rangle_1 \otimes |\alpha_{20}\rangle_2$  for mode  $\hat{a}_1$ , i.e.,  $e^{-itg\hat{H}_{int}}|1\rangle_1 \otimes |\alpha_{20}\rangle_2 \approx |1\rangle_1 \otimes |\alpha_{20}\rangle_2 - i2tg\alpha_{20}\sqrt{6}|3\rangle_1 \otimes |\alpha_{20}\rangle_2$ . So the analysis with the formation of odd SCLSs is similar to the analysis performed for even SCLSs and skipped.

We believe that the results of the theoretical analysis performed in this paper on the formation of SCLSs during the SPDC process can be a valuable quantum resource for the problems of quantum sensing [4, 5] and optical qubit formation [8, 40]. In particular, it is interesting to understand the relation of the non-classicality we observe to the Bell-type non-classicality, which in general has a different nature [41].

Such states can also be used in the Mach-Zehnder interferometers [2–5] and can potentially be used to identify small perturbations if they are coupled to the perturbation medium. In addition, our results may stimulate the development of a continuous variable quantum information theory beyond the well-established Gaussian case [37].

It should be noted that the further study of SCLSs is getting more attention of researchers [42], e.g., in identification of the optimal time for generation of SCLSs in the fundamental mode.

The SCLSs proposed in this paper could be observed experimentally with the help of quantum optical homodyne tomography [39]. Moreover, the formation of such states is based on second-order susceptibility and contains a relatively large number of average photons  $> 2$ , where less pump mode intensity is required to be compared to third-order susceptibility.

## ACKNOWLEDGMENTS

We thank Prof. Anatoly V. Masalov for discussions on obtained results and providing valuable inputs.

- 
- [1] V. V. Dodonov, I. A. Malkin, and V. I. Man'ko, Even and odd coherent states and excitations of a singular oscillator, *Physica* **72**, 597 (1974).
  - [2] A. Shukla and B. C. Sanders, Superposing compass states for asymptotic isotropic sub-planck phase-space sensitivity, *Physical Review A* **108**, 043719 (2023).
  - [3] F. Toscano, D. A. Dalvit, L. Davidovich, and W. H. Zurek, Sub-planck phase-space structures and heisenberg-limited measurements, *Physical Review A* **73**, 023803 (2006).
  - [4] D. Salykina and F. Khalili, Sensitivity of quantum-enhanced interferometers, *Symmetry* **15**, 10.3390/sym15030774 (2023).
  - [5] R. Singh and A. E. Teretenkov, Quantum sensitivity of squeezed schrodinger cat states, *Physics Open* **18**, 100198 (2024).
  - [6] G. S. Agarwal, *Quantum optics* (Cambridge University Press, 2013).
  - [7] P. T. Cochrane, G. J. Milburn, and W. J. Munro, Macroscopically distinct quantum-superposition states as a bosonic code for amplitude damping, *Physical Review A* **59**, 2631 (1999).
  - [8] Y. Yamamoto, T. G. Leleu, S. Ganguli, and H. Mabuchi, Coherent ising machines—quantum optics and neural network perspectives, *Applied Physics Letters* **117**, 160501 (2020).
  - [9] W. H. Zurek, Sub-planck structure in phase space and its relevance for quantum decoherence, *Nature* **412**, 712

- (2001).
- [10] S. L. Braunstein and P. van Loock, Quantum information with continuous variables, *Rev. Mod. Phys.* **77**, 513 (2005).
- [11] D. V. Sychev, A. E. Ulanov, A. A. Pushkina, M. W. Richards, I. A. Fedorov, and A. I. Lvovsky, Enlargement of optical schrodinger, s cat states, *Nature Photonics* **11**, 379 (2017), arXiv:1609.08425 [quant-ph].
- [12] S. P. Nikitin and A. V. Masalov, Quantum state evolution of the fundamental mode in the process of second-harmonic generation, *Quantum Optics: Journal of the European Optical Society Part B* **3**, 105 (1991).
- [13] R. Singh, G. G. Amosov, and A. V. Masalov, Schrodinger cat states in the process of generation of the second optical harmonic, in *XII International Symposium on Photonic Echo and Coherent Spectroscopy (FEKS-2021) in the Memory of Prof. V. V. SAMARTSEV: Collection of Abstracts. Kazan, 25-30 October (2021)*, edited by E. B. P. A. Kalachev and A. N. E. Edition] (Moscow: Trovant, ISBN: 978-5-89513-501-3, (in Russian), 2021) pp. 52–54.
- [14] A. Ourjountsev, R. Tualle-Brouri, J. Laurat, and P. Grangier, Generating optical schrodinger kittens for quantum information processing, *Science* **312**, 83 (2006).
- [15] M. S. Podoshvedov, S. A. Podoshvedov, A. P. Alodjants, and S. P. Kulik, Promising quantum engineering of optical even/odd schrodinger cat states, *Vestnik Yuzhno-Uralskogo Gosudarstvennogo Universiteta. Seriya Matematika. Mekhanika. Fizika* **14**, 77 (2022).
- [16] M. Kitagawa and Y. Yamamoto, Number-phase minimum-uncertainty state with reduced number uncertainty in a Kerr nonlinear interferometer, *Phys. Rev. A* **34**, 3974 (1986).
- [17] A. Miranowicz, R. Tanas, and S. Kielich, Generation of discrete superpositions of coherent states in the anharmonic oscillator model, *Quantum Optics: Journal of the European Optical Society Part B* **2**, 253 (1990).
- [18] A. V. Baeva, N. G. Veselkova, N. I. Masalaeva, and I. V. Sokolov, Measurement-assisted non-gaussian gate for schrodinger cat states preparation: Fock resource state versus cubic phase state, *European Physical Journal D* **78**, 12 (2024), arXiv:2307.06349 [quant-ph].
- [19] D. Walls and G. Milburn, *Quantum Optics* (Springer Berlin Heidelberg, 2008).
- [20] G. P. Agrawal and C. L. Mehta, Dynamics of parametric processes with a trilinear hamiltonian, *Journal of Physics A Mathematical General* **7**, 607 (1974).
- [21] V. N. Beskrovnyi and A. S. Chirkin, Generation of squeezed light at doubled frequency in a ring resonator, in *Atomic and Quantum Optics: High-Precision Measurements*, Society of Photo-Optical Instrumentation Engineers (SPIE) Conference Series, Vol. 2799, edited by A. S. Chirkin and S. N. Bagayev (1996) pp. 212–219.
- [22] A. V. Belinsky and R. Singh, Simultaneous nonlinear conversion of light in periodically poled crystals, *Quantum Electronics* **48**, 611 (2018).
- [23] D. F. Walls and R. Barakat, Quantum-mechanical amplification and frequency conversion with a trilinear hamiltonian, *Physical Review A* **1**, 446 (1970).
- [24] D. F. Walls and C. T. Tindle, Non-linear quantum effects in optics, *Journal of Physics A Mathematical General* **5**, 534 (1972).
- [25] T. Gantsog, R. Tanaś, and R. Zawodny, Quantum phase fluctuations in parametric down-conversion with quantum pump, *Optics Communications* **82**, 345 (1991).
- [26] R. Tanas and T. Gantsog, Number and phase quantum fluctuations in the down-conversion with a quantum pump, *Quantum Optics* **4**, 245 (1992).
- [27] R. Tanas, T. Gantsog, and R. Zawodny, Number and phase quantum fluctuations in second harmonic generation, *Quantum Optics* **3**, 221 (1991).
- [28] G. Drobný and I. Jex, Statistics of field modes in the process of k-photon down-conversion with a quantized pump, *Physical Review A* **45**, 4897 (1992).
- [29] T. Gantsog, R. Tanaś, and R. Zawodny, Collapses and revivals of quantum phase fluctuations in the down-conversion with quantum pump, *Acta Phys. Slov.* **43**, 74 (1993).
- [30] J. R. Johansson, P. D. Nation, and F. Nori, QuTiP: An open-source Python framework for the dynamics of open quantum systems, *Computer physics communications* **183**, 1760 (2012).
- [31] J. Johansson, P. Nation, and F. Nori, QuTiP 2: A Python framework for the dynamics of open quantum systems, *Computer Physics Communications* **184**, 1234 (2013).
- [32] V. Dmitriev, G. Gurzadyan, and D. Nikogosyan, *Handbook of Nonlinear Optical Crystals*, Springer Series in Optical Sciences (Springer Berlin Heidelberg, 1999).
- [33] H. Wiseman and G. Milburn, *Quantum Measurement and Control* (Cambridge University Press, New York, 2010).
- [34] H.-P. Breuer and F. Petruccione, *The Theory of Open Quantum Systems* (Oxford University Press, New York, 2002).
- [35] M. Strinati and C. Conti, Non-gaussianity in the quantum parametric oscillator, *Phys. Rev. A* **109**, 063519 (2024).
- [36] W. Vogel and D.-G. Welsch, *Quantum optics* (John Wiley & Sons, 2006).
- [37] A. S. Holevo, *Quantum Systems, Channels, Information* (De Gruyter, Berlin, Boston, 2019).
- [38] A. Divochiy, F. Marsili, D. Bitauld, A. Gaggero, R. Leoni, F. Mattioli, A. Korneev, V. Seleznev, N. Kaurova, O. Minaeva, *et al.*, Superconducting nanowire photon-number-resolving detector at telecommunication wavelengths, *Nature Photonics* **2**, 302 (2008).
- [39] S. Paul, Arman, S. Lakshmi-bala, P. Panigrahi, S. Ramanan, and V. Balakrishnan, Optimal sensing of photon addition and subtraction on nonclassical light, arXiv:2409.12881 (2024).
- [40] S. Lloyd and S. L. Braunstein, Quantum computation over continuous variables, *Phys. Rev. Lett.* **82**, 1784 (1999).
- [41] I. V. Volovich, Cauchy–schwarz inequality-based criteria for the non-classicality of sub-poisson and antibunched light, *Physics Letters A* **380**, 56 (2016).
- [42] V. Gorshenin, Preparation of schrodinger cat quantum state using parametric down-conversion interaction, arXiv:2407.05759 (2024).